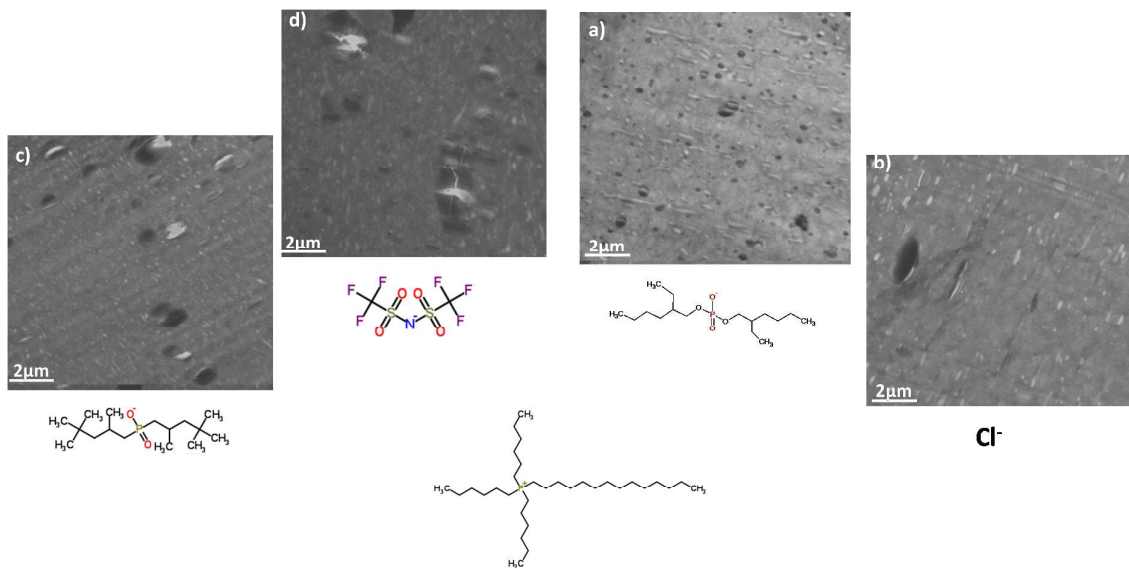




**Ionic Liquids-Lignin combination: An innovative way to improve mechanical behaviour and water vapour permeability of eco-designed biodegradable polymer blends**

Journal:	<i>RSC Advances</i>
Manuscript ID:	RA-ART-10-2014-011919.R1
Article Type:	Paper
Date Submitted by the Author:	22-Nov-2014
Complete List of Authors:	Livi, Sébastien; Cornell University, MS&E Bugatti, Valeria; University of Salerno, Department of Industrial Engineering Maréchal, Manuel; CNRS, LEPMI (UMR 5279) Soares, Bluma; IMA, Duchât, Jannick; INSA de Lyon, IMP GERARD, Jean-François; IMP-INSA, Barra, Guilherme; Federal University of Santa Catarina, Mechanical Engineering Department



Effect of ILs on the morphologies of biodegradable polymers

## ARTICLE

# Ionic Liquids-Lignin combination: An innovative way to improve mechanical behaviour and water vapour permeability of eco-designed biodegradable polymer blends

Cite this: DOI: 10.1039/x0xx00000x

Received 00th January 2012,  
Accepted 00th January 2012

DOI: 10.1039/x0xx00000x

[www.rsc.org/](http://www.rsc.org/)Sébastien Livi<sup>a\*</sup>, Valeria Bugatti<sup>b</sup>, Manuel Marechal<sup>c</sup>, Bluma .G. Soares<sup>d</sup>,  
Guilherme M.O. Barra<sup>e</sup>, Jannick Duchet-Rumeau<sup>a</sup>, Jean-François Gérard<sup>a</sup>

In this work, the potential use of lignin combined with ionic liquids (ILs) has been investigated on the final properties of biodegradable polymer blends. Poly(butylene-adipate-co-terephthalate)/polylactide/lignin (PBAT/PLA/Lig) were melt blending in one pot by using phosphonium ionic liquids as new additives. The effect of incorporating 16 wt% of lignin and PLA and 1 wt% of ILs into PBAT matrix has been explored on the mechanical behaviour, the water vapour permeability, the thermal stability as well as the morphologies of PBAT/PLA/Lig/IL blends. In all cases, the lignin/ionic liquid combination leads to a good mechanical performance coupled with a dramatic increase in water barrier properties. In addition, transmission electron microscopy (TEM) analysis has been used to investigate the influence of ILs on the different morphologies of these sustainable polymer blends.

## A Introduction

In the world of polymeric materials, academic and industrial research has focused on the development of sustainable composites or nanocomposites based on renewable resources such as cellulose, soy stalk, starch and lignin for various applications such as food packaging or compostable films [1-2]. To achieve this, many authors have investigated the combination of biodegradable polymer blends [3-6]. Thus, polylactide (PLA) was the subject of special attention due to these excellent properties. In fact, PLA have a good stiffness and good water vapour barrier properties. However, its low strain at break prevents its use for packaging industries [7-8]. For this reason, different ways have been developed in the literature: i) PLA is commonly blended with more ductile biodegradable polymers such as poly(butylene-adipate-co-terephthalate) (PBAT), poly(butylene-succinate-co-adipate), polycaprolactone or poly(butylene succinate) [9-11]; ii) the incorporation of ionic liquids as plasticizers of PLA matrix [12-13]; and iii) the use of renewable resources as reinforcing agents of flexible polymers [14-21].

For the first route, the problem of miscibility between polymers results in phase-separated morphologies [22-24]. In this case, the use of copolymers, ionomers or the incorporation of nanoparticles (layered silicates, silica) are required to stabilize the morphologies of polymer blends and to improve the mechanical performances of polymer mixtures [25-28]. For example, different authors have demonstrated that the use of treated layered silicates leads to an

increase of the Young Modulus coupled with a slight improvement of only 2-3 % of the strain at break [29]. Other authors have preferred to use in situ reactive compatibilization in the presence of chain extender with also mixed results [30].

In recent years, few studies have highlighted the preparation of ductile polylactide by using phosphonium or imidazolium ionic liquids [31]. Indeed, ionic liquids are known for their excellent properties such as their low vapor pressure, their excellent thermal stability and their good versatility as well as their infinite cation/anion combination [32-36]. Thus, Chen et al have demonstrated that the use of 20 wt. % of ILs induces an increase of the elongation at break (60 % instead of 5 %) [12]. The limiting factor of this method is the high price of ILs.

Finally, other authors have studied the influence of renewable resources (biodegradable fibers or lignocellulose fillers) as reinforcements of biodegradable polymers such as aromatic or aliphatic copolyesters [37-39]. For example, Gordobit et al have investigated the influence of lignin on the mechanical properties of PLA matrix. In all cases, the use of lignin has conducted to the reduction of Young Modulus as well as a slight increase in elongation at break (7% instead of 3%). Other authors have studied the grafting of PLA onto unmodified lignin by using ring-opening polymerization. These changes have resulted in increases in the glass transition temperatures (85 °C instead of 45 °C) but also in the mechanical properties (Young Modulus and tensile strength).

As lignin is a waste product of the biorefinery and paper industries, the lignin which is one of the most abundant and less expensive

resources has been used in thermoplastics and biopolymers with mixed results. For all these reasons, our research group has focused on improving the final properties of PBAT/PLA blends by using lignin (Lig) as reinforcing agent and the ionic liquids as modulable multifunctional additives in function of their chemical nature. In addition, to best of our knowledge, no work has studied the lignin/IL combination on the water vapor permeability, the mechanical behavior and the morphologies of biodegradable poly(butylene-adipate-co-terephthalate)/polylactide mixtures.

## B Experimental

### B.1 Materials

The polylactide used in this study, denoted 2002D, is an amorphous PLA from NatureWorks® with a reported T<sub>g</sub> of 61 °C, a density of 1.25 g/cm<sup>3</sup> and a melt flow index of 10-25g/10 min (Molecular weight of 200000 g/mol). Moreover, PLA has a D content of 4.25%, a residual monomer content of 0.3%. The PBAT was supplied by BASF under the trade name of Ecoflex and have a density of 1.26 g/cm<sup>3</sup> (Molecular weight of 72000 g/mol). Lignin alkali with low sulfonate content was supplied by Aldrich (Molecular weight of 28000 g/mol).

The four ionic liquids based on phosphonium cations combined with different counter anions and different molar masses were provided by Cytec Industries Inc. They include:

- Trihexyl(tetradecyl)phosphonium chloride denoted IL-Cl (M<sub>m</sub> = 519 g/mol)
- Trihexyl(tetradecyl)phosphonium bis-2,4,4-(trimethylpentyl)phosphinate named IL-TMP (M<sub>m</sub> = 773 g/mol)
- Trihexyl(tetradecyl)phosphonium bistriflimide named IL-TFSI (M<sub>m</sub> = 764 g/mol)
- Trihexyl(tetradecyl)phosphonium bis-2-(ethylhexyl)phosphate named IL-EHP (M<sub>m</sub> = 805 g/mol)

The structures and nomenclatures of phosphonium ionic liquids are presented in Table 1.

**Table 1.** Designation of used ionic liquids

Commercial name	Abbreviation	Cation structure	Anion structure
CYPHOS® IL104	IL-TMP		
CYPHOS® IL109	IL-TFSI		
CYPHOS® IL101	IL-Cl		Cl <sup>-</sup>
CYPHOS® IL349	IL-EHP		

### B.2 Processing and instrumental characterization of the PBAT/PLA/Lignin with and without ILs

Nanocomposites based on PBAT/PLA/Lignin/ILs (64/16.5/16.5/1 wt.%) were prepared under nitrogen atmosphere using a 15 g-capacity DSM micro-extruder (Midi 2000 Heerlen, The Netherlands) with co-rotating screws (L/D ratio of 18). The procedure is as follows: In the first time, PBAT/PLA/lignin blends are mechanically pre-mixed and incorporated into the micro-extruder. Then, phosphonium ionic liquids are injected into the extruder. The mixture was sheared under nitrogen atmosphere for about 3 min with a 100 rpm speed at 160 °C and injected in a 10 cm<sup>3</sup> mould at 30 °C to obtain dumbbell-shaped specimens. All the compositions of the biodegradable polymer mixtures are presented in Table 2.

**Table 2.** Composition of the PBAT/PLA, PBAT/PLA/Lignin with and without ILs

Designation	m(PBAT):m(PLA):m(Lig):m(IL)
PBAT-PLA	80 :20
PBAT/PLA/Lig	80 :20 :20
PBAT/PLA/Lig/IL-Cl	80 :20 :20 :1
PBAT/PLA/Lig/IL-TMP	80 :20 :20 :1
PBAT/PLA/Lig/IL-TFSI	80 :20 :20 :1
PBAT/PLA/Lig/IL-EHP	80 :20 :20 :1

*Thermogravimetric analyses (TGA) of biodegradable polymer blends* were performed on a Q500 thermogravimetric analyser (TA instruments). The samples were heated from 30 to 600 °C at a rate of 20 °C.min<sup>-1</sup> under nitrogen flow. TGA analyzes were conducted on two samples.

*DSC measurements (DSC)* of PBAT, PLA and polymer mixtures were performed on a Q20 (TA instruments) from 30 to 200°C. The samples were kept for 1 min at 200°C to erase the thermal history before being heated or cooled at a rate of 10 °C.min<sup>-1</sup> under nitrogen flow of 50 mL.min<sup>-1</sup>. The crystallinity was calculated with the heat of fusion for PLA of 93 J/g [40] and with the heat of fusion for PBAT of 114 J/g [41]. DSC measurements were performed on two samples.

*Transmission electron microscopy (TEM)* was carried out at the Center of Microstructures (University of Lyon) on a Philips CM 120 microscope with an accelerating voltage of 80 kV. The samples were cut using an ultramicrotome equipped with a diamond knife, to obtain 60-nm-thick ultrathin sections. Then, the sections were set on copper grids.

*Uniaxial Tensile Tests* were carried out on a MTS 2/M electromechanical testing system (load cell of 10kN) at 22±1°C and 50±5% relative humidity at crosshead speed of 50 mm.min<sup>-1</sup>. The strain was calculated from the crosshead displacement. The tensile tests were performed on five samples (dumbbell-shaped AFNOR H3, thickness 2 mm). The samples were conditioned at 22±1°C and 50±5% relative humidity during 24h prior to tensile testing.

*Small-Angle Neutron Scattering (SANS)* experiments were carried on a small angle spectrometer (PAXY, Léon Brillouin Laboratory, Saclay, France). Two sample-to-detector distances (SDD) and neutron wavelengths ( $\lambda$ ) were used to cover a magnitude of the scattering vector modulus  $q$  from 0.09 to 4.2 nm<sup>-1</sup> ( $\lambda=1.2$  nm, SDD = 3 m, and  $\lambda=0.5$  nm, SDD = 1 m). The resulting level of the scattering intensity at the high  $q$  values is of the order of magnitude of the experimental background. The incoherent contributions of the polymer and ionic liquid phases were subtracted.

*Water Vapor Sorption experiments* were performed on PBAT/PLA/Lignin films with and without ionic liquids by compression molding at 160 °C using a conventional McBain spring balance system, which consists of a glass water-jacketed chamber serviced by a high vacuum line for sample degassing and permeant removal. Inside, the chamber samples were suspended from a helical quartz spring supplied by Ruska Industries, Inc. (Houston, TX) and had a spring constant of 1.52544 cm/mg. The temperature was controlled to  $30 \pm 0.1$  °C by a constant temperature water bath. Sorption was measured as a function of the relative pressure,  $a=P/P_0$ , where  $P$  is the actual pressure (in mmHg) of the experiment, and  $P_0$  the saturation pressure at 30°C for water (32 mmHg) during 24 h. The samples were exposed to the penetrant at fixed pressures ( $a=0.53$ ), and the spring position was recorded as a function of time using a cathetometer. Data averaged on three samples. Diffusion coefficients and equilibrium mass uptake were extracted from these kinetic sorption data. Water vapor sorption were performed on three samples.

Measuring the increase of weight with time, for the samples exposed to the vapour at a given partial pressure, it is possible to obtain the equilibrium value of sorbed vapour,  $C_{eq}$  ( $g_{solvent}/100 g_{polymer}$ ). Moreover, in the case of Fickian behaviour, that is a linear dependence of sorption on square root of time, it is possible to derive the mean diffusion coefficient from the linear part of the reduced sorption curve, reported as  $C_t/C_{eq}$  versus square root of time [42], by the Eq. (1)

$$\frac{C_t}{C_{eq}} = \frac{4}{d} \left( \frac{Dt}{\pi} \right)^{1/2}$$

Eq (1)

where  $C_t$  is the penetrant concentration at the time  $t$ ,  $C_{eq}$  is the equilibrium value,  $d$  (in cm) is the thickness of the sample and  $D$  ( $cm^2/s$ ) the average diffusion coefficient.

From the first part of the isotherms, when the sorption can be assumed ideal and following the Henry's law, we derived a sorption parameter ( $S$ ):

$$S = \frac{dC_{eq}}{dp}$$

Eq (2)

where  $p$  is the partial pressure of the water vapour. All the samples showed a Fickian behaviour during the sorption of water vapour at activity  $a=0.53$ . Using Eq. (1), it was possible to derive the average diffusion coefficient,  $D$  ( $cm^2/s$ ), at every fixed vapour activity ( $a=P/P_0$ ) and the equilibrium concentration of solvent into the sample,  $C_{eq}$  ( $g_{solvent}/100g_{polymer}$ ). The solubility coefficient,  $S$ , in  $cm^3$  (STP)/( $cm^3 \cdot atm$ ), can be calculated from  $C_{eq}$  as follows:

$$S = \frac{C_{eq}}{100} \frac{\rho}{MW_{penetrant}} \frac{22,414}{P}$$

Eq (3)

Where  $\rho$  is the sample density,  $P$  is the penetrant pressure in atm,  $MW_{penetrant}$  is the penetrant molecular weight in g/mol, and 22,414 is a conversion factor.

The permeability of the samples to the vapour is given by the product of sorption and diffusion:

$$P = S \cdot D$$

Eq (4)

## C Results and discussion

### C.1 Morphologies of sustainable polymer blends

Transmission electron microscopy is the suitable tool to reveal the existence of PLA as a separated phase into the PBAT matrix according to the difference in electronic densities. The concomitant differences of scattering length densities are probed by neutron scattering. Indeed, it permits to characterize the interfaces of the phase nanosegregation between both polymer phases. This technique is relevant to characterize such samples and to determine if there is any structuration in the used  $q$ -range between 0.09 to  $4.2 \text{ nm}^{-1}$ . In addition, the influence of the lignin as well as the effect of the chemical nature of the ionic liquid was studied on morphologies of PBAT-PLA blends.

#### C.1.1. Effect of lignin on PBAT-PLA blends

To highlight the different morphologies of the binary blend PBAT-PLA and the ternary blend PBAT-PLA-Lig, TEM micrographs are reported in Figure 1. Moreover, the distribution of the PLA phases in PBAT-PLA mixtures with and without the presence of lignin was determined by image analysis (Figure 2).

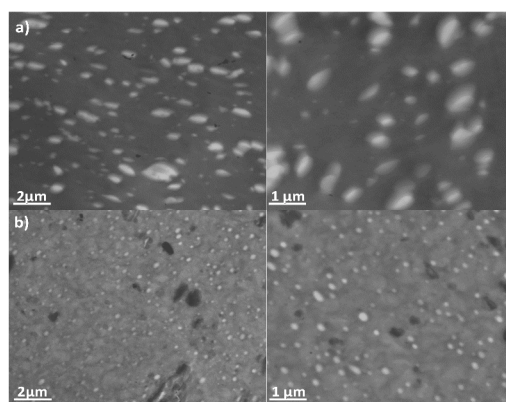


Figure 1. TEM micrographs of (a) PBAT-PLA and (b) PBAT-PLA-Lig mixtures

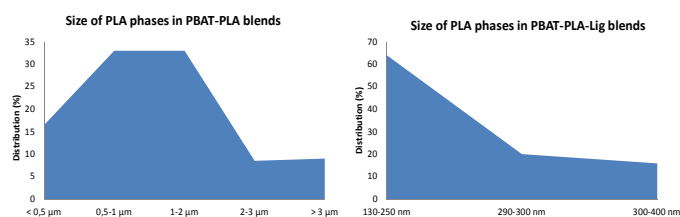
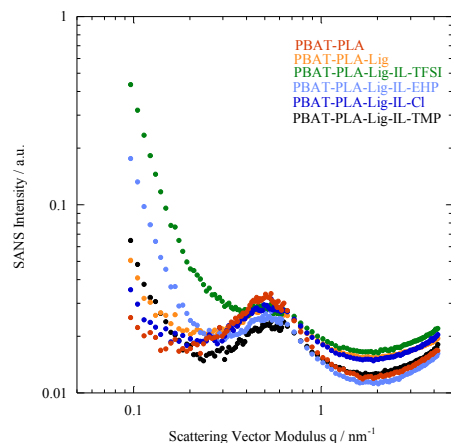


Figure 2. Size distribution of PLA domains obtained for the PBAT-PLA blends with and without lignin using Imaje J software

In the case of PBAT-PLA blends without lignin, TEM images confirmed the presence of two immiscible phases [43-44]. In addition, PLA domains are homogeneously distributed in PBAT matrix and had diameters between 0.5 and 3 μm. However, the size distribution of PLA domains obtained confirmed a slight affinity of the PLA with the PBAT matrix. Indeed, compared to systems based on polyolefin blends, diameters of several tens of microns are commonly observed [22, 45]. Then, these results are consistent with the literature on PLA-PBAT mixtures where diameters in the 0.7 – 1.5 μm are generally determined [9].

The presence of lignin in the PBAT-PLA blends led in a significant improvement of the dispersion of PLA phases in PBAT matrix coupled to a significant reduction in the size of the PLA nodules from 1-2 microns to less than 400 nanometers. Thus, 65% of the PLA domains showed diameters in the 130 – 250 nm.



**Figure 3.** Scattered intensity versus scattering-vector modulus  $q$  for the PBAT-PLA, the PBAT-PLA-Lignin with the IL-Cl, IL-EHP, IL-TMP and IL-TFSI.

The neutron scattering permits to bulky probe the multiscale structure of the samples (Figure 3). The broad peak obtained for all samples corresponds to the distance between the crystallites of the semi-crystalline polymer phases, PBAT and PLA. In the present case, this correlation length due to the intercrystallite is 11.9 nm, the related  $q$  being equal to  $0.53 \text{ nm}^{-1}$  obtained using a Gaussian model to fit the peak. The long-range structure is different with and without lignin since the upturn at low  $q$  is not the same. The upturn starting at higher  $q$  for the PBAT-PLA-Lig confirms that the correlation length due to the PLA-rich phase decreases with the presence of lignin.

Furthermore, the TEM micrographs show clearly the good solubility of the lignin in PBAT matrix except the presence of few lignin aggregates. This decrease of the PLA nodule sizes is a phenomenon commonly encountered in polymer blends. In fact, lignin (biodegradable filler) acts as a nanoparticle which stabilize the mixture [46-47]. Thus, an accumulation of lignin at the interphase induced to a formation of a barrier around the PLA phase preventing the coalescence of PLA nodules therefore leading to the formation of small particles [47-48]. According to the literature, Nayak et al have demonstrated that the addition of nanoclays in PBAT/thermoplastic starch (TPS) led to the reduction in particle size of TPS [49].

In summary, the use of lignin as biodegradable filler improved the compatibility between PBAT and PLA along with finer distribution of PLA domains (130 – 250 nm).

### C.1.2 Effect of the chemical nature of the counter anion on PBAT-PLA-Lig mixtures

Then, the influence of the chemical nature of the counter anion was investigated on the morphologies of ternary polymer blends composed of PBAT-PLA-Lignin. TEM micrographs of PBAT-PLA-Lig with the presence of phosphonium ionic liquids denoted IL-Cl, IL-TFSI, IL-TMP and IL-EHP are presented in Figure 4 and Figure 5.

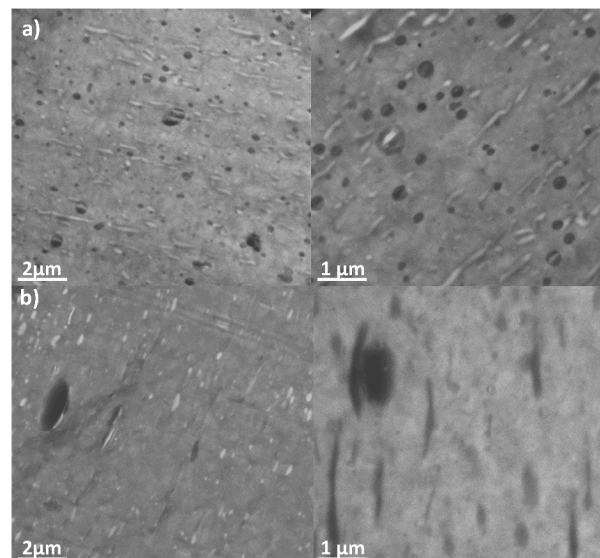


**Figure 4.** TEM micrographs of (a) PBAT/PLA/Lig/IL-EHP and (b) PBAT/PLA/Lig/IL-Cl blends

In the case of PBAT/PLA/Lig/IL-EHP and PBAT/PLA/Lig/IL-Cl blends, the use of only 1 wt % of IL-EHP and IL-Cl has generated completely different morphologies. First, the presence of phosphonium ILs has changed the morphologies of the PLA domains in form of elongated droplets. This phenomenon is not new and has been widely observed and described in the ternary blends comprising thermoplastics and layered silicates. In fact, several parameters have an effect on the morphology of the dispersed phase: i) the shear forces which tend to deform the droplets as is the case here (Figure 4), ii) the interfacial tension forces that oppose to the deformation. In summary, the size of the dispersed phase as well as the shape are dependent of the competition between coalescence and break up during the melt mixing [50-51]. Like block copolymers, ionomers or nanoparticles, these results highlighted the role of compatibilizing agent of phosphonium ionic liquids and open new perspectives in polymer blends [22, 46-47].

For lack to confirm the morphology of the segregation in this  $q$ -range, the neutron scattering (Figure 3) permit to confirm that certain ionic liquids lead to a new structuration: the IL-EHP and the IL-Cl. These new interfaces between both polymer phases are well defined since the beginning of the slope is a  $q^{-4}$  power. With the other ionic liquids, IL-TFSI and IL-TMP, it is difficult to conclude on the structuration without information at lower  $q$  even if, with the beginning of the upturns, we can confirm the nanosegregation at lower  $q$ , i.e. with higher correlations lengths.

Moreover, a second phenomenon is evidenced by the TEM micrographs (Figure 4). The incorporation of the phosphonium ILs also induced a change of shape and a reduction in particle sizes of lignin. Unlike the PBAT-PLA-Lignin mixture with the presence of large aggregates of lignin, a finer dispersion as well as a reduction of particle size of lignin are observed. Thus, for the PBAT/PLA/Lig/IL-EHP where an image analysis is possible, 80 % of the lignin particles showed diameters in the 30 - 220 nm.

These results can be explained by the strong interaction between the phosphate and chloride anions with the hydroxyl groups (OH) of lignin. According to the literature on the cellulose/IL mixtures, the presence of hydroxyl groups on the lignin leads to the formation of intra- and intermolecular hydrogen bonding's while the addition of ionic liquids combined with anions such as chloride or acetate promotes strong hydrogen bonds resulting in partial dissolution of lignin particles under melt mixing [52-54].

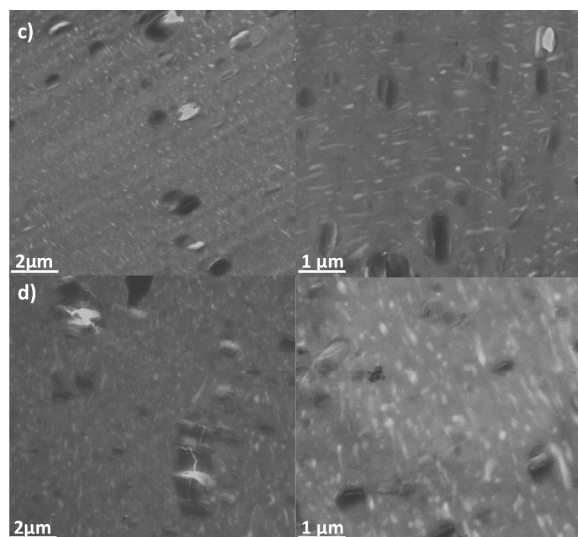


**Figure 5.** TEM micrographs of (c) PBAT/PLA/Lig/IL-TMP and (d) PBAT/PLA/Lig/IL-TFSI blends

Regarding the PBAT/PLA/Lignin filled with IL-TMP and IL-TFSI, a significant decrease of the PLA domain sizes as well as an excellent dispersion were observed. In the opposite, TEM micrographs have revealed the formation of lignin aggregates ( $> 1-2 \mu\text{m}$ ). These results show clearly the best affinity of IL-TMP and IL-TFSI with the PLA matrix and can be explained by their basicity. In fact, Livi et al have demonstrated that the use of IL-TFSI and IL-TMP in PP/PA6 blends have interactions with the terminal acid groups of the polyamide 6 [22].

In conclusion, the different morphologies observed are controlled by the chemical nature of the counteranion. Thus, depending on the nature of the matrix, it becomes possible to generate the desired structuration for specific applications.

## C.2. Thermal properties of biodegradable polymer blends

The degradation mechanisms and the influence of the ionic liquids on the thermal behavior of PBAT-PLA-Lig blends have been investigated by thermogravimetric analysis (TGA). The evolution of the weight loss as a function of a temperature performed on pure ionic liquids, lignin and biodegradable polymer mixtures containing 1 wt% of phosphonium ionic liquids is shown in Figure 6 and Figure 7.

### C.2.1. Thermal stability of ionic liquids

The effect of the chemical nature of the counter anion on the thermal stability of trihexyl(tetradecylphosphonium) ILs is presented in Figure 6.

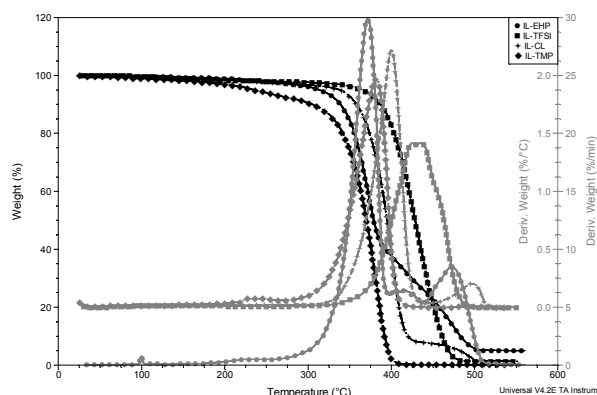


**Figure 6.** Weight loss as a function of temperature (TGA) of the (●) IL-EHP, (■) IL-TFSI, (+) IL-Cl, (◆) IL-TMP (heating rate :  $20 \text{ }^\circ\text{C}\cdot\text{min}^{-1}$ , nitrogen atmosphere).

The combination of the counter anion associated with the phosphonium cation has a key role on the thermal behavior of ILs. In fact, the use of TFSI anion (fluorinated anion) combined with phosphonium cation leads to an increase of degradation temperature of  $70 \text{ }^\circ\text{C}$  compared to the phosphonium salts denoted IL-Cl, IL-EHP and IL-TMP. This result has been demonstrated in the literature by different authors [55-57]. Thus, Awad et al have demonstrated that the imidazolium salts combined with fluorinated anions such as  $\text{PF}_6^-$  or  $\text{BF}_4^-$  led to an increase of the thermal stability of  $100 \text{ }^\circ\text{C}$  compared to halide salts [34]. Other authors have also studied the thermal stability of phosphonium ILs combined with hydrophilic anion such as decanoate or phosphinate anions and they have highlighted the lower thermal stability of these anions. In conclusion, the most thermally stable phosphonium ILs are IL-TFSI > IL-Cl > IL-TMP > IL-EHP.

### C.2.2. Thermal behaviour of the nanocomposite blends

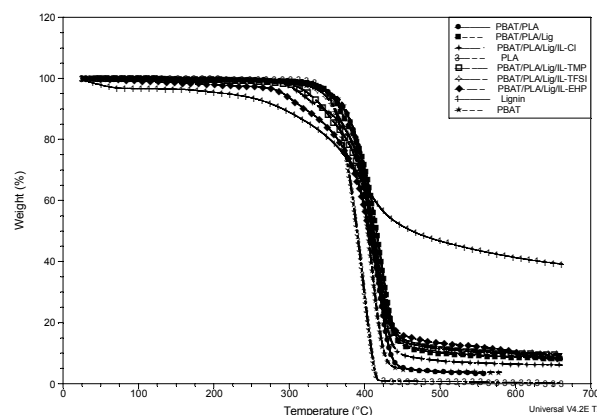


**Figure 7.** Weight loss as a function of temperature (TGA) of the (\*) PBAT, (3) PLA, (1) Lignin, (●) PBAT-PLA, (■) PBAT-PLA-Lig, (+) PBAT/PLA/Lig/IL-Cl, (□) PBAT/PLA/Lig/IL-TMP, (◇) PBAT/PLA/Lig/IL-TFSI and (◆) PBAT/PLA/Lig/IL-EHP (heating rate :  $20 \text{ }^\circ\text{C}\cdot\text{min}^{-1}$ , nitrogen atmosphere).

In all cases, the TGA curves highlight an excellent thermal behavior of the biodegradable polymer blends ( $> 300 \text{ }^\circ\text{C}$ ). However, the addition of lignin leads to a slight decrease in the thermal stability of the polymer blends. In fact, a degradation peak at  $370 \text{ }^\circ\text{C}$  is observed in the TGA curves. This peak corresponds to the degradation of the lignin which has a lower thermal stability than PBAT-PLA blend (Figure 7). Then, the addition of phosphonium

ionic liquids accelerates the degradation of the PBAT-PLA-Lig mixtures. Similarly, these results are explained by the intrinsic stability of ionic liquids: IL-TFSI and IL-Cl which are the most thermally stable ILs moderate the thermal degradation ( $T_{10\%} = 360$  °C compared to 370 °C for PBAT-PLA) of the biodegradable blends while IL-TMP and IL-EHP lead to a degradation temperatures of 340 °C and 315 °C, respectively.

### C.2.3 Differential scanning calorimetry (DSC)

The DSC thermograms of the virgin PBAT, PLA as well as the PBAT-PLA and PBAT-PLA-Lig without and with ILs are presented in Figure 8. Melting temperature ( $T_m$ ), glass transition temperature ( $T_g$ ), crystallization temperature ( $T_c$ ), cold crystallization temperature ( $T_{cc}$ ), and melting enthalpies ( $\Delta H_m$ ) are summarized in Table 3 and Table 4. Furthermore, based on the corresponding enthalpies of 100% crystalline of PBAT (114 J/g) and PLA (93 J/g), the degree of crystallinity have been calculated for the PBAT and PLA phases in order to highlight the influence of lignin and ionic liquids on each of the two phases.

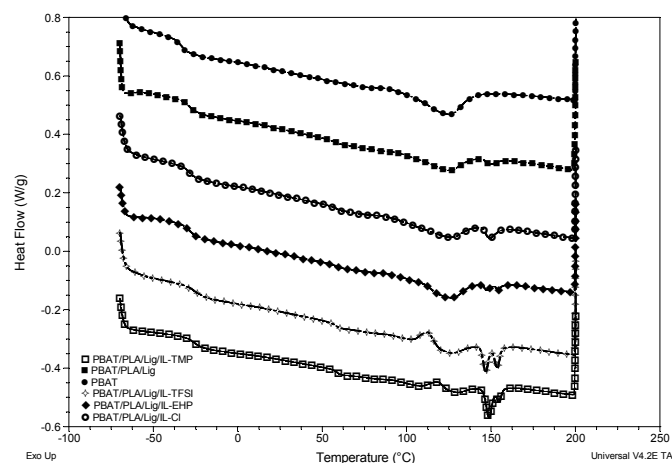


**Figure 8.** DSC thermograms (second heating) of the (●) PBAT, (■) PBAT-PLA-Lig, (○) PBAT/PLA/Lig/IL-Cl, (□) PBAT/PLA/Lig/IL-TMP, (+) PBAT/PLA/Lig/IL-TFSI and (◆) PBAT/PLA/Lig/IL-EHP

**Table 3.** Differential scanning calorimetry analyses of PBAT/PLA blends and PBAT/PLA/Lignin with and without ILs (second heating cycle)

Samples	$T_g$ (°C)	$T_g$ (°C)	$T_m$ (°C)	$T_c$ (°C)	$T_{cc}$ (°C)
PBAT	-33±0.3	-	123±0.5	64±1.1	-
PLA	-	61.9±0.4	-	-	-
PBAT/PLA	-28.6±0.3	61.2±0.2	116.1±0.4	65±0.5	-
PBAT/PLA/Lig	-27.9±0.4	58.6±0.5	124.6±0.4	78±0.8	-
PBAT/PLA/Lig/IL-Cl	-29.3±0.2	57.9±0.1	124.7±0.3	70±1.2	-
PBAT/PLA/Lig/IL-TMP	-26.6±0.4	58.8±0.4	129.1±0.3	77±0.4	117±0.2
PBAT/PLA/Lig/IL-TFSI	-26.7±0.2	57.1±0.3	123.2±0.3	74±0.8	114±0.2
PBAT/PLA/Lig/IL-EHP	-29.3±0.6	58.6±0.3	124.9±0.5	71±0.3	-

**Table 4.** Differential scanning calorimetry analyses of PBAT/PLA blends and PBAT/PLA/Lignine with and without ILs (second heating cycle)

Samples	$\Delta H_m$ (J/g)	$\Delta H_m$ (J/g)	% (PBAT)	% (PLA)
	PBAT	PLA	crystallinity	crystallinity
PBAT	13.5±0.7	-	12	-
PLA	-	-	-	-
PBAT/PLA	15±1.1	-	13	-
PBAT/PLA/Lig	10.5±0.4	3.6±0.2	9.2	3.8
PBAT/PLA/Lig/IL-Cl	5.8±0.3	7.9±0.2	5.1	8.4
PBAT/PLA/Lig/IL-TMP	12.2±0.4	21.8±0.4	10.7	23.2
PBAT/PLA/Lig/IL-TFSI	7.3±0.4	21.8±0.2	6.4	23.2
PBAT/PLA/Lig/IL-EHP	11.6±0.2	4.2±0.3	10.2	4.4

#### C.2.3.1. Effect of the renewable resource on the thermal properties of PBAT-PLA blends

About neat polymer matrices, the second heating scan of PBAT showed a glass transition temperature at -33 °C and an endothermic peak at 123 °C whereas for the PLA sample, only a glass transition temperature of 61.9 °C appeared [58-59]. Then, in the case of PBAT/PLA blends, two glass transition temperatures (-26.5 °C for PBAT, 61.2 °C for PLA) and an endothermic peak at 116 °C were observed which suggest that the PBAT has no influence on the crystallization of the PLA. According to the literature, the same phenomenon is observed for PLA-PBAT blends (80-20) [9, 24]. In fact, Jiang et al have investigated the influence of the incorporation of PBAT (0-20 wt%) in PLA matrix and whatever the amount of PBAT, only the melting peak of PLA is obtained [9].

In the opposite, the incorporation of 20 wt% of lignin in PBAT-PLA mixtures led to the appearance of a small melting peak at 148 °C highlighting the presence of a new crystalline structure induced by lignin [9, 49]. In addition, the introduction of lignin causes a slight increase in the glass transition temperature (-28.6 °C to -27.9 °C) as well as a significant increase of the melting temperature (117 °C to 124 °C) of the PBAT matrix. These results clearly demonstrate the interactions between the hydroxyl groups of the lignin and the (CH-COO)<sub>2</sub> of the PBAT. In fact, other authors have also observed this phenomenon [49]. For example, Nayak et al showed that the addition of modified clays in PBAT/starch blends leads to higher  $T_g$  and  $T_m$  and the authors explained this result by the reduction of the size of thermoplastic starch in PBAT. This assumption is well confirmed by the TEM micrographs described above (Figure 1) where the addition of lignin induced a strong decrease in the size of PLA domains.

#### C.2.3.2. Effect of phosphonium ionic liquids on the thermal behaviour of PBAT-PLA-Lig mixtures

When the ionic liquids are introduced in the PBAT-PLA-Lig mixtures, two different behaviors are observed. In the case of phosphonium ILs denoted IL-TMP and IL-TFSI, the addition of a small amount of ILs leads to increase of the glass transition temperature of 2 °C and an increase of the melting temperature (+7 °C) of PBAT matrix. Moreover the appearance of an exothermic peak at 114-117 °C corresponding to the cold crystallization highlights a reorganization of the amorphous phase of the PLA matrix into crystalline ones [9, 43]. These results are confirmed by the appearance of melting temperature of about 148 °C and by the determination of the melting enthalpy ( $\Delta H_m$ ) which corresponds to the data of the PLA matrix [24]. The same observations were made by Signori et al in PLA-PBAT blends [24]. However, in both cases, the presence of IL-TMP and IL-TFSI leads to the appearance of two melting peaks at 148 and 153 °C. According to the literature, the melting peak at 153 °C corresponds to the pure PLA while the peak

at lower temperature (148 °C) suggests the presence of a new crystalline structure induced by the lignin/IL combination. Thus, IL-TMP and IL-TFSI coupled with lignin led to heterogeneous nucleation effect characterized by a decrease of the crystallization temperature (78 °C to 75 and 73 °C for IL-TMP and IL-TFSI, respectively). According to the morphologies observed in Figure 4, these two ionic liquids generate the formation of lignin aggregates which similarly act as the nanoclays. Indeed, the presence of lignin aggregates induces the immobilization of PBAT chains [49]. Regarding IL-Cl and IL-EHP, no exothermic peak were observed whereas a slight decreases of the glass transition temperatures of the biodegradable polymer blends (-28.6 °C to -30 °C) were obtained which confirms a slight plasticizer role of these ionic liquids. In addition, the glass transition temperatures of PLA slightly decrease in all cases which confirm the key role of lignin and phosphonium ionic liquids as interfacial agents of PBAT/PLA blends.

In conclusion, the chemical nature of the anion of the ILs plays a key role in the phenomena of crystallization of the biodegradable polymer blends and depending therefrom, the final properties of the polymeric materials will be adjustable in function of the desired applications.

### C.3 Mechanical performance of biodegradable polymer blends

To reveal the effect of phosphonium ionic liquids on the mechanical performance of PBAT/PLA/Lignine blends, the uniaxial tensile properties were investigated. The Young Modulus and the fracture properties are shown in Table 5.

Sample	Young Modulus (MPa)	Strain at break (%)	Stress (MPa)
PBAT	47±1	510±17	23±1
PLA	2500±100	4±2	62±5
PBAT/PLA	115±5	540±20	20±3
PBAT/PLA/Lig	150±10	410±15	21±1
PBAT/PLA/Lig/IL-Cl	140±5	650±30	23±1
PBAT/PLA/Lig/IL-EHP	120±10	800±50	23±2
PBAT/PLA/Lig/IL-TMP	240±20	520±10	20±1
PBAT/PLA/Lig/IL-TFSI	190±20	450±22	20±1

**Table 5.** Mechanical data from tensile tests performed on neat PBAT, PLA, PBAT/PLA and PBAT/PLA/lignine blends filled with different phosphonium ILs.

Firstly, the addition of lignin in PBAT/PLA mixture leads to an increase of the Young Modulus (+ 30%) as well as a decrease of the strain at break (- 24%). In fact, lignin particles act as reinforcing agent and this mechanical behaviour is explained by the morphology obtained in Figure 1. Secondly, the presence of phosphonium ILs induces different mechanical behaviours: IL-TMP and IL-TFSI induce significant increases in stiffness compared to PBAT/PLA/Lignin blend (+ 60% and + 30%, respectively) combined with slight increases of the strain at break (+ 27% and + 10%). In the opposite, IL-Cl and IL-EHP cause an increase in the strain at break (+ 60% and + 95%) without reducing the Young Modulus. These results can be explained by the influence of ionic liquids on the thermal properties of polymer blends but also on the morphologies observed by transmission electron microscopy. Indeed, the crystallization of the PLA matrix generated by the presence of IL-TMP and IL-TFSI as well as the presence of lignin aggregates in polymer blends explain the mechanical performance of these blends. Whereas the use of phosphonium ILs denoted IL-EHP and IL-Cl have a plasticizer effect confirmed by the slight decrease

of the glass transition temperature (-2 °C) obtained by DSC. In addition, the good affinity of the lignin with phosphate and chloride anions which resulted in a decrease of the particle size of lignin could explain this better stretchability of the PBAT/PLA/Lignin blends. In terms of tensile strength, the incorporation of PLA but also lignin combined with the ionic liquids does not induce any change.

These results are promising and highlight the beneficial effect of ionic liquids as new compatibilizers of biopolymers. Thus, the use of a renewable resource combined with only 1 wt% of ILs may be an alternative to the block copolymers, the nanoparticles and the ionomers, commonly used in the literature [25-29].

### C.4. Water barrier properties of biodegradable polymer blends

To highlight the water barrier properties of biopolymer blends, the water sorption ( $C_{eq}$  and  $S$ ) as well as the diffusion ( $D$ ) and the permeability ( $P$ ) of the neat PBAT and PBAT/PLA/Lignine without and with phosphonium ionic liquids IL-Cl, IL-TMP, IL-TFSI and IL-EHP are presented in Table 6.

**Table 6.** Water sorption, water diffusion and water permeability for neat PBAT and PBAT/PLA/Lig blends with and without ionic liquids.

Sample	Water Sorption $C_{eq}$ (g/100g)	Water Diffusion $D$ (cm <sup>2</sup> /sec)	Water Permeability (cc <sub>STP</sub> /cm <sup>3</sup> *atm <sup>-1</sup> )*(cm <sup>2</sup> /sec)
PBAT	2.37±0.0035	2.26*10 <sup>-8</sup> ±1.05*10 <sup>-10</sup>	3.32*10 <sup>-8</sup> ±1.40*10 <sup>-10</sup>
PLA	0.45±0.0024	7.75*10 <sup>-8</sup> ±1.45*10 <sup>-10</sup>	2.17*10 <sup>-8</sup> ±1.20*10 <sup>-10</sup>
PBAT/PLA	0.16±0.0012	9.63*10 <sup>-9</sup> ±2.80*10 <sup>-11</sup>	9.82*10 <sup>-10</sup> ±1.30*10 <sup>-11</sup>
PBAT/PLA/Lig	0.26±0.0015	1.13*10 <sup>-9</sup> ±1.10*10 <sup>-10</sup>	2.15*10 <sup>-10</sup> ±2.00*10 <sup>-11</sup>
PBAT/PLA/Lig/IL-Cl	0.21±0.0010	6.09*10 <sup>-10</sup> ±3.00*10 <sup>-11</sup>	9.50*10 <sup>-11</sup> ±8.00*10 <sup>-12</sup>
PBAT/PLA/Lig/IL-EHP	0.16±0.0016	8.04*10 <sup>-10</sup> ±4.00*10 <sup>-11</sup>	9.56*10 <sup>-11</sup> ±2.00*10 <sup>-11</sup>
PBAT/PLA/Lig/IL-TMP	0.25±0.0021	7.46*10 <sup>-10</sup> ±1.2*10 <sup>-11</sup>	1.38*10 <sup>-10</sup> ±2.00*10 <sup>-11</sup>
PBAT/PLA/Lig/IL-TFSI	0.14±0.0013	1.62*10 <sup>-9</sup> ±2.9*10 <sup>-11</sup>	1.68*10 <sup>-10</sup> ±1.01*10 <sup>-11</sup>

Concerning the two neat matrices PBAT and PLA, the data highlighted that the water sorption of the PLA matrix is lower than PBAT (2.37 instead of 0.45g/100g) while the water molecules diffuse more rapidly in the polylactide matrix. Thus, the incorporation of the PLA and its excellent distribution in the PBAT matrix resulted in a significant increase in water barrier properties. Then, the incorporation of lignin and various ionic liquids denoted IL-Cl, IL-TMP, IL-TFSI and IL-TFSI causes a dramatic decrease of the water sorption compared to the neat PBAT matrix. In fact, the reductions are included from 89 % to 94 %. In the case of lignin, these results are due to the strong interactions between the hydroxyl groups of the lignin and the (CH-COO)<sub>2</sub> of the PBAT matrix. While for polymer blends containing phosphonium ILs, the hydrophobic nature of the phosphonium cation characterized by the presence of long alkyl chains explains the decrease of the water sorption [60-61]. According to the literature, the surface energies of the phosphonium ILs are in the range of 30.2 – 30.7 mN.m<sup>-1</sup> which is similar to surface energies of polyolefins [62-63]. Thus, Livi et al have demonstrated that addition of 2 wt% of ionic liquid in poly(butylene-adipate-co-terephthalate) led decreases from 40 to 80 % of the water sorption [64]. Regarding the water diffusion in the polymer matrix,

the excellent distribution of PLA domains (droplets or fibers) obtained for PBAT/PLA/Lig with and without ILs induces the formation of a tortuous path which has the effect to delay the diffusion of small molecules of water through PBAT matrix ( $6.09 \times 10^{-10}$  for PBAT/PLA/Lig/IL-Cl instead of  $2.26 \times 10^{-8}$  cm<sup>2</sup>/sec for neat PBAT) [65-66]. However, IL-EHP and IL-Cl which lead to the dissolution of lignin aggregates combined to an excellent good dispersion of PLA phases have a more pronounced effect on slowing the diffusion of water. This trend is also confirmed for the water permeability coefficients where the largest reductions are obtained for the PBAT/PLA/Lig blends containing IL-EHP and IL-Cl. Indeed, permeability values of  $9.56 \times 10^{-11}$  and  $9.50 \times 10^{-11}$  are obtained compared to values of  $1.38 \times 10^{-10}$  and  $1.68 \times 10^{-10}$  for IL-TMP and IL-TFSI, respectively.

According to the literature on the water vapor permeation (WVP) of biopolymer filled with nanoparticles or polymer blends such as PBAT/TPS, PBAT/starch, the results obtained in this study are very promising and open a new route of compatibilization of immiscible polymeric materials [67-68]. In fact, regarding the use of nanoparticles as layered silicates (MMT) in the field of polymer nanocomposites, the incorporation of 5 % to 10 % of organically modified clays are required to mixed results (-20%, -30%) [32, 69]. Recently, Livi et al demonstrated that the incorporation of 5 wt% of imidazolium-treated montmorillonites (MMT-I) causes a reduction of 60 % of the water vapour barrier properties [32]. However, this way generates several limitations: i) the surface treatment of clay, ii) the increase of the viscosity which has an effect on the processing of polymer nanocomposites and iii) the control of the dispersion of nanoparticles must be optimum to obtain the best final properties. Other authors have also studied the influence of surfactant or plasticizers in PBAT/starch blends but only slight decreases of the WVP are obtained (7-15 %) [67, 70].

In conclusion, the combined use of lignin and ionic liquid leads to a significant increase in the water vapour barrier properties of biodegradable mixtures. Thus, PBAT/PLA/Lig blends with the use of ILs as compatibilizers can be used for compostable film applications.

## Conclusions

In this study, various phosphonium ionic liquids have been used for the first time as compatibilizing agents for biodegradable polymer blends reinforced with renewable resource such as lignin. Then, the influence of the chemical nature of the counter anion of the ionic liquid was investigated on the morphology as well as the final properties such as thermal, mechanical and barrier properties of polymer blends. Thus, we have identified two different behaviors depending on the ionic liquid used: IL-TMP, IL-EHP, IL-TFSI and IL-Cl. IL-Cl and IL-EHP lead to a significant decrease in the size of PLA domains and lignin which clearly highlighting a better affinity of phosphate and chloride anions with lignin. In contrast, due to their basicity, IL-TMP and IL-TFSI have a better affinity with the terminal acid groups of polylactide chains compared to lignin where the presence of aggregates was observed. Nevertheless, in all cases, the combination IL-lignin generates significant improvements in the mechanical performance and in barrier properties of polymeric materials. In conclusion, this work opens new perspectives in the field of food packaging but also in the processing of compostable films for agricultural land.

## Acknowledgement

The authors thank Alain Lapp and François Boué as local contacts on the PAXY (LLB) spectrometer.

## Notes and references

<sup>a</sup> Université de Lyon, F-69003, Lyon, France; INSA Lyon, F-69621, Villeurbanne, France; CNRS, UMR 5223, Ingénierie des Matériaux Polymères.

<sup>b</sup> Department of Industrial Engineering, University of Salerno, Via Ponte Don Melillo 1, 84084-Fisciano (SA), Italy.

<sup>c</sup> CNRS, LEPMI, F-38000 Grenoble; Univ. Grenoble Alpes, LEPMI, F-38000 Grenoble, France.

<sup>d</sup> Universidade Federal do Rio de Janeiro, Instituto de Macromoléculas, 21941-598, Rio de Janeiro-RJ, Brazil.

<sup>e</sup> Universidade Federal de Santa Catarina, Departamento de Engenharia Mecânica, Florianópolis, SC, Brazil.

- 1 M. Okamoto and B. John, *Prog. Polym. Sci.*, 2013, **38**, 1487–1503.
- 2 P. X. Ma, *Mater. Today*, 2004, **7**, 30–40.
- 3 P. Bordes, E. Pollet and L. Averous, *Prog. Polym. Sci.*, 2009, **34**, 125–155.
- 4 P. Tormala, S. Vainionpää, J. Kilpikari and P. Rokkanen, *Biomaterials*, 1987, **8**, 42–45.
- 5 K. Anselme, B. Flautre, P. Hardouin, M. Chanavaz, C. Ustariz and M. Vert, *Biomaterials*, 1993, **14**, 44–50.
- 6 R. de Juana, A. Jauregui, E. Calahorra and M. Cortazar, *Polymer*, 1996, **37**, 3339–3345.
- 7 F.D. Kopinke, M. Remmler, K. Mackenzie, M. Moder, O. Wachsen, *Polym. Degrad. Stab.*, 1996, **53**, 329–42.
- 8 V. Taubner, R. Shishoo, *J. Appl. Polym. Sci.*, 2001, **79**, 2128–35.
- 9 L. Jiang, M.P. Wolcott, J. Zhang, *Biomacromolecules*, 2006, **7**, 199–207.
- 10 Y.H. Na, Y. He, X. Shuai, Y. Kikkawa, Y. Doi, Y. Inoue, *Biomacromolecules*, 2002, **3**, 1179–86.
- 11 T. Furukawa, H. Sato, R. Murakami, J.M. Zhang, Y.X. Duan, I. Nodal, *Macromolecules*, 2005, **38**, 6445–54.
- 12 B-K. Chen, T-Y. Wu, Y-M. Chang, A.F. Chen, *Chem. Eng. Journal*, 2013, **215**, 2013, 886–893.
- 13 K.I. Park, M. Xanthos, *Polym. Degrad. Stab.*, 2009, **94**, 834–844.
- 14 R. Mani, M. Bhattacharya, *Eur. Polymer J.*, 2001, **37**, 515–526.
- 15 J. Li, Y. He, Y. Inoue, *Polym. Int.*, 2003, **52**, 949-955.
- 16 C. Reti, M. Casetta, S. Duquesne, S. Bourbigot, R. Delobel, *Polymers for adv. Tech.*, 2008, **19**, 628-635.
- 17 O. Gordobil, I. Egues, R. Llano-Ponte, J. Labidi, *Polym. Degrad. Stab.*, 2014, **108**, 330-338.
- 18 I. Spiridon, K. Leluk, A.M. Resmerita, R.N. Darie, *Composites Part B: Eng.*, 2015, **69**, 342-349.
- 19 R. Zhang, X. Xiao, Q. Tai, H. Huang, J. Yang, Y. Hu, *J. Appl. Polym. Sci.*, 2013, **127**, 4967-4973.
- 20 T-L. Chung, J.V. Olsson, R.J. Li, C.W. Franck, R.M. Waymouth, S.L. Billington, E.S. Sattely, *ACS Sust. Chem. Eng.*, 2013, **1**, 1231-1238.
- 21 F. Le Digabel, L. Averous, *Carbohydr. Polym.*, 2006, **23**, 537–545.
- 22 M. Yousfi, S. Livi, J. Duchet-Rumeau, *Chem. Eng. Journal*, 2014, **255**, 513–524.
- 23 E.-J. Choi and J.-K. Park, *Polym. Degrad. Stab.*, 1996, **52**, 321–326.

- 24 F. Signori, M-B. Coltelli, S. Bronco, *Polym. Degrad. Stab.*, 2009, **94**, 1, 74–82.
- 25 F. Ide, A. Hasegawa, *J. Appl. Polym. Sci.*, 1974, **18**, 963–974.
- 26 J.M. Willis, B.D. Davis, *Polymer Eng. & Sci.*, 1988, **28**, 1416–1426.
- 27 L. Elias, F. Fenouillot, J.C. Majeste, P. Cassagnau, *Polymer*, 2007, **48**, 6029–6040.
- 28 J. Chen, Y-Y. Shi, J-H. Yang, N. Zhang, T. Huang, Y. Wang, *Polymer*, 2013, **54**, 464–471.
- 29 S.S. Ray, M. Bousmina, A. Maazouz, *Polymer Eng. & Sci.*, 2006, **46**, 1121–1129.
- 30 V. Ojijo, S. Sinha Ray, R. Sadiku, *ACS Appl. Mater. Interfaces*, 2013, **5**, 4266–4276.
- 31 K. Park, J-U. Ha, M. Xanthos, *Polymer Eng. & Sci.*, 2010, **50**, 1105–1110.
- 32 S. Livi, G. Sar, V. Bugatti, E. Espuche, J. Duchet-Rumeau, *RSC Adv*, 2014, **4**, 26452.
- 33 S. Livi, V. Bugatti, L. Estevez, J. Duchet-Rumeau, E.P. Giannelis, *Journal of Colloid and Interface Science*, 2012, **388**, 123–129.
- 34 W. H. Awad, J.W. Gilman, M. Nyden, R.H. Harris, T.E. Sutto, J. Callahan, P.C. Trulove, H.C. Delong, D.M. Fox, *Thermochim. Acta*, 2004, **409**, 13.
- 35 S. Livi, J. Duchet-Rumeau, J-F. Gerard, *Eur. Polym. J.*, 2011, **47**, 1361–1369.
- 36 J. Zhu, A. B. Morgan, F. J. Lamelas, C.A. Wilkie, *Chem Mater*, 2001, **13**, 3774.
- 37 S.T. Lim, Y.H. Hyun, H.J. Choi, *Chem Mater*, 2002, **14**, 1839.
- 38 M.F. Koenig, S.J. Huang, *Polymer*, 1995, **36**, 1877.
- 39 I. Tomka, R.F. Stepto, B. Dobler, *Eur. Pat. Appl*, 1987, 88810130.0.
- 40 Tsuji H, Ikada Y. *Macromol Chem Phys*, 1996, **197**, 3483.
- 41 R. Herrera, L. Franco, A. Rodriguez-Galan and J. Puiggali, *J. Polym. Sci., Part A: Polym. Chem.*, 2002, **40**, 4141–4157.
- 42 W. R. Vieth and M. A. Amini, *Generalized dual sorption theory, in Permeability of plastics films and coatings*, ed. H.B. Hopfenberg, Plenum Press, New York, 1974.
- 43 M. Kumar, S. Mohanty, S.K. Nayak, M. R. Parvaiz, *Biosource Tech.*, 2010, **101**, 8406–8415.
- 44 R. Al-Itry, K. Lamnawar, A. Maazouz, *Rheo. Acta*, 2014, **53**, 501–517.
- 45 S.S. Ray, M. Bousmina, *Macromol. Rapid Commun*, 2005, **26**, 450–455.
- 46 F. Fenouillot, P. Cassagnau, J.C. Majeste, *Polymer*, 2009, **50**, 1333–1350.
- 47 F. Laoutid, D. François, Y. Paint, L. Bonnaud, P. Dubois, *Macromol. Mat. Eng.*, 2013, **298**, 328–338.
- 48 F. Laoutid, E. Estrada, R.M. Michel, L. Bonnaud, A.J. Mueller, P. Dubois, *Polymer*, 2013, **54**, 3982–3993.
- 49 S.K. Nayak, *Polymer-Plastics Tech. Eng.*, 2010, **49**, 1406–1418.
- 50 J. Huitric, P. Médéric, M. Moan, T. Aubry, *J. Rheology*, 2009, **53**, 1101–1109.
- 51 Grace, H. P., *Chem. Eng. Commun*, 1982, **14**, 225–277.
- 52 R.P. Swatloski, S.K. Spear, J.D. Holbrey, R.D. Rodgers, *J. Am. Chem. Soc*, 2002, **124**, 4974.
- 53 Y. Fukasa, K. Hayashi, M. Wada, H. Ohno, *Green Chem*, 2008, **10**, 44.
- 54 H. Ohno, Y. Fukasa, *Chem Lett*, 2009, **38**, 2.
- 55 C.G. Begg, M.R. Grimmett, P.D. Wethey, *Aust. J. Chem*, 1973, **26**, 2435.
- 56 C. Byrne, T. McNally, *Macromol. Rapid Commun*, 2007, **28**, 780.
- 57 S. Livi, J. Duchet-Rumeau, T. N. Pham, J-F. Gérard, *J. Colloid Interface Sci.*, 2011, **354**, 555–562.
- 58 N. López-Rodríguez, A. López-Arraiza, E. Meaurio, J.R. Sarasua, *Polymer Eng. & Sci.*, 2006, **46**, 1299–1308.
- 59 F. Chivrac, Z. Kadlecová, E. Pollet, L. Avérous, *J Polym Environ*, 2006, **14**, 393–401.
- 60 P.J. Carvalho, C.M.S.S. Neves, J.A.P. Coutinho, *J. Chem. Eng.Data*, 2010, **55**, 3807–3812.
- 61 H.F.D. Almeida, J.A. Lopes-da-Silva, M.G. Freire, J.A.P. Coutinho, *J. Chem. Thermodyn*, 2013, **57**, 372–379.
- 62 C.M. Hansen, A. Beerbower, *Kirk-Othmer Encyclopedia of Chemical Technology*, second ed., vol. **889**, Ed. Interscience, New York, 1971.
- 63 S. Livi, J. Duchet-Rumeau, T. N. Pham, J-F. Gérard, *J. Colloid Interface Sci.*, 2010, **349**, 424–433.
- 64 S. Livi, V. Bugatti, B.G. Soares, J. Duchet-Rumeau, *Green Chem.*, 2014, **16**, 3758–3762.
- 65 C. Labruyere, G. Gorrasi, F. Monteverde, M. Alexandre and Ph. Dubois, *Polymer*, 2009, **50**, 3626–3637.
- 66 G. Gorrasi, M. Tortora, V. Vittoria, E. Pollet, B. Lepoittevin, M. Alexandre and Ph. Dubois, *Polymer*, 2003, **44**, 2271–2279.
- 67 J.B. Olivato, M.V.E. Grossmann, F. Yamashita, D. Eiras, L.A. Pessan, *Carbohydr. Polym.*, 2012, **87**, 2614–2618.
- 68 I.F.E. Silva, F. Yamashita, C.M.O. Muller, S. Mali, J.B. Olivato, A.P. Bilck, M.V.E. Grossmann, *Int. Journal of Food Sci. & Tech.*, 2013, **48**, 1762–1769.
- 69 D. Mondal, B. Bhowmick, M. M. R. Mollick, D. Maity, N. R. Saha, V. Rangarajan, D. Rana, R. Sen, D. Chattopadhyay, *J. Appl. Polym. Sci.*, 2014, **7**, 131.
- 70 R. P. H. Brandelero, F. Yamashita and M. V. E. Grossmann, *Carbohydr. Polym.*, 2010, **82**, 1102.